Rania Zaky and Ahmed Fekri*

Solvent-free mechanochemical synthesis of Zn(II), Cd(II), and Cu(II) complexes with 1-(4-methoxyphenyl)-4-(2-(1-(pyridin-2-yl)-ethylidene)hydrazinyl)-1H-pyrrole-3-carbonitrile

https://doi.org/10.1515/gps-2017-0057
Received May 6, 2017; accepted October 13, 2017; previously published online December 23, 2017

Abstract: Zn(II), Cd(II), and Cu(II) complexes with 1-(4-methoxyphenyl)-4-(2-(1-(pyridin-2-yl)ethylidene)-hydrazinyl)-1H-pyrrole-3-carbonitrile (HP) were produced by using ball milling as a mechanochemical technique. The mode of chelation for the isolated complexes was illustrated by several spectroscopic techniques. Also, a computational study was estimated to prove the geometry of the isolated complexes by applying a density function theory method. In addition, its biological activity (antimicrobial and DNA binding) was evaluated.

Keywords: DFT; DNA; mechanochemical synthesis; Schiff bases.

1 Introduction

In bioinorganic chemistry, the Schiff bases family as well as their transition metal complexes plays a significant role. These stimulating ligand systems have various active donor sites in heterocyclic rings, such as pyridine moiety, which provide the architectural attractiveness of these coordination complexes [1–4]. The transition metal complexes of these ligands advanced because of their structural flexibility, chelating ability, and magnetic properties along with several interesting electrical and pharmacological activities, such as antitumor, antimalarial, antibacterial, antituberculosis, and antiviral actions [5–8].

In contrast, not much research has been performed on the DNA binding of such complexes because of the interaction between DNA and metal complexes, which is thoroughly linked to their potential pharmaceutical and biological activities. Scientific research on the DNA binding of metal complexes is essential in the improvement of novel DNA molecular probes and therapeutic reagents [9–11].

Therefore, in view of the important biological properties of the 2-acetyl pyridine nuclei, attaching the abovementioned ring system to the pyrrole moiety to search for potentially improved biological actions has been considered. Therefore, zinc (II), cadmium (II), and copper (II) metal complexes were prepared using an environmentally friendly, simplistic, solvent-less, and clean synthesis using a ball-milling technique, which is considered as an important mechanochemical method for the preparation of organic as well as inorganic compounds [12–17].

***Corresponding author: Ahmed Fekri,** Department of Chemistry, Faculty of Science, Mansoura University, Mansoura 35516, Egypt, e-mail: taiiam1978@gmail.com. http://orcid.org/0000-0001-9733-1161
Rania Zaky: Department of Chemistry, Faculty of Science, Mansoura University, Mansoura 35516, Egypt

2 Materials and methods

2.1 Equipment

The Retsch MM 2000 swing ball-mill (Retsch, Haan, Germany) (at a frequency of 20,225 Hz) was used for the preparation of solid complexes. The Mercury 300 MHz is an nuclear magnetic resonance (NMR) spectrometer synthetic by Varian (Varian, Palo Alto, CA, USA) that was used to detect the ^{1}H and ^{13}C NMR spectra in dimethyl sulfoxide (DMSO). Fourier transform infrared spectroscopy was done with a Mattson 5000 (Madison, WI, USA), and the spectra was determined in the 4000–400 cm^{-1} region. A Philips X-Pert X-ray diffractometer (Philips, Eindhoven, the Netherlands) was used to detect the patterns of X-ray diffraction (XRD) for the isolated compounds. The Bruker EMX Spectrometer (Bruker, Karlsruhe, Germany) (modulation frequency = 100 kHz working at 9.78 GHz in the X-band) was used to record the electron spin resonance (ESR) spectrum. A scanning electron microscope (SEM; JEOL JSM 6510lv) (JEOL, Tokyo, Japan) was used to investigate the surface structures using its high-quality stereoscopic image clarity and magnification capabilities. The mass spectra of prepared ligands was determined *via* "DI analysis Shimadzu QP-2010" with ion source (200°C) temperature scan speed 526, start end (m/z) (50–300), (70 eV) & ionization mode (EI). Magnetic susceptibility balance (Johnson Matthey, Wayne, PA, USA) was used to detect the magnitude of the magnetic moment. A Shimadzu UV 240 spectrophotometer (P/N 204-58000, Kyoto, Japan) was used to determine the electronic spectra in the 200–900 nm region of Cu(II) complex in DMSO as a solvent. A Perkin-Elmer 2400 Series II Analyzer (Perkin-Elmer, Waltham, MA, USA) was used to decide the percentages of carbon, hydrogen, and nitrogen. All reagents used were supplied by Sigma-Aldrich, Cairo, Egypt and software used was ChemDraw Professional 15.0, Perkin-Elmer, USA.

2.2 Synthesis of 1-(4-methoxyphenyl)-4-(2-(1-(pyridin-2-yl) ethylidene)hydrazinyl)-1H-pyrrole-3-carbonitrile (HP)

HP was synthesized by refluxing the 4-hydrazinyl-1-(4-methoxy phenyl)-1H-pyrrole-3-carbonitrile (2.28 g; 10.0 mmol) with 2-acetylpyridine (1.22 g; 10.0 mmol) in 1 ml glacial acetic acid (1 M)

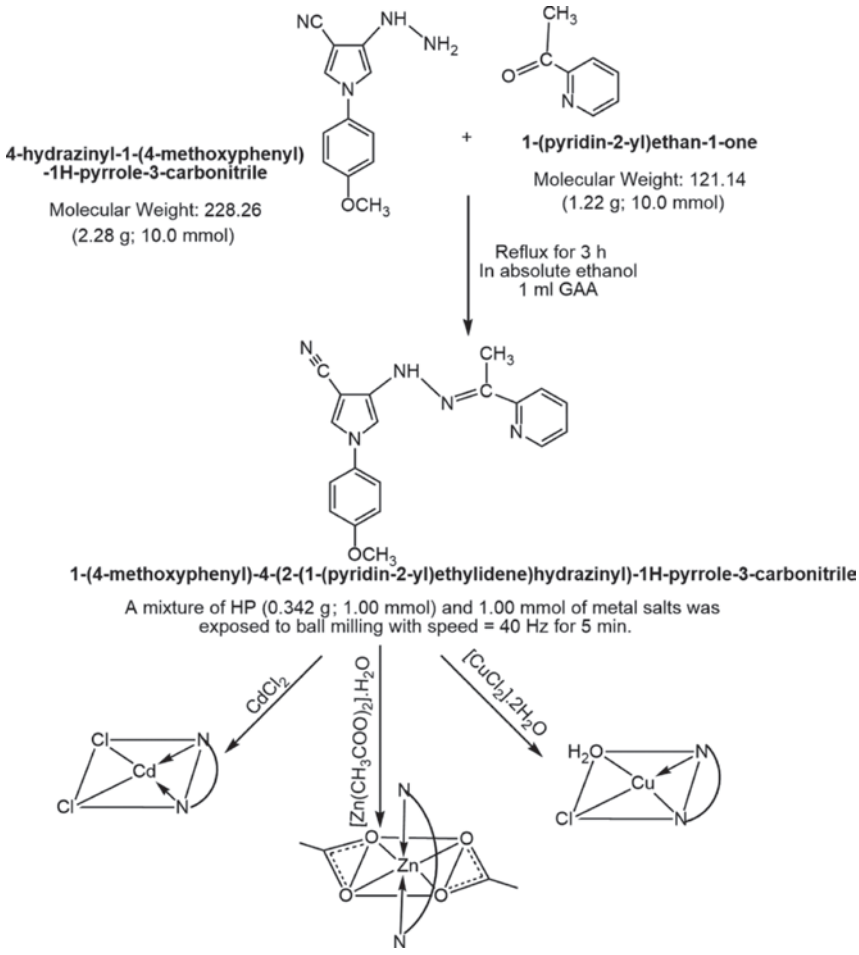

Figure 1: The synthesis of HP and its $[Zn(HP)(OAc)_2]$, $[Cd(HP)Cl_2]$, and $[Cu(P)(H_2O)Cl]$ complexes.

for 3 h. The buff ppt formed was then filtered off and washed with ethyl alcohol.

2.3 Synthesis of complexes

A mix of HP (0.342 g; 1.00 mmol) and 1.00 mmol of $[Zn(CH_3COO)_2] \cdot H_2O$, $CdCl_2$, or $[CuCl_2] \cdot 2H_2O$ metal salts was exposed to ball milling at a speed of 40 Hz for 5–9 min. Thin-layer chromatography established the reaction progress (Figure 1).

2.4 Experimental data

1-(4-methoxyphenyl)-4-(2-(1-(pyridin-2-yl)ethylidene)-hydrazinyl)-1H-pyrrole-3-carbonitrile (HP) (1, $C_{19}H_{17}N_5O$) Found (buff solid): C = 68.85; H = 5.12; N = 21.10. Calc.: C = 68.87; H = 5.12; N = 21.13. Yield: 78%. m.p.: 208°C. ^{1}H NMR: d = 10.46 (s, NH), 7.18–8.74 (m, 10H/aromatic protons), 2.32 (s, 3H, –N=C–CH_3/methyl group), 3.83 (s, 3H/–OCH_3). ^{13}C NMR (200 MHz, DMSO-d6): d (ppm) main signals: 147 $(C=N)_{Azo}$; 156 $(C=N)_{py}$; 13 (CH_3). IR: $\bar{\upsilon}$ = 3250 (NH), 1652 $(C=N)_{azo}$, 802 $(C=N)_{py}$. MS: $C_{19}H_{17}N_5O$, Calc.: m/z = 331.19; found: m/z = 332.14.

$[Zn(HP)(OAc)_2]$ (2, $ZnC_{23}H_{23}N_5O_5$) Found (yellowish-white solid): %C = 53.64; %H = 4.49; %N = 21.12, %Zn = 12.66 Calc.: %C = 53.68; %H = 4.51; %N = 21.15, %Zn = 12.70. Yield: 88%. m.p.: >300°C. ^{1}H NMR: d = 10.57 (s, NH), 7.24–8.83 (m, 10H/aromatic protons), 2.30 (s, 3H, –N=C–CH_3/methyl group), 3.78 (s, 3H/–OCH_3). ^{13}C NMR: d (ppm) main signals: 140 $(C=N)_{Azo}$; 149 $(C=N)_{py}$); 18 (CH_3COO); 10 (CH_3). IR: $\bar{\upsilon}$ = 3253 (NH), 1640 $(C=N)_{azo}$, 803 $(C=N)_{py}$, 511 (Zn-O), 464 (Zn-N). Molar conductivity: Λ_m = 6 ohm^{-1} cm^2 mol^{-1} (in DMSO).

$[Cd(HP)Cl_2]$ (3, $CdC_{19}H_{17}N_5OCl_2$) Found (yellowish-white solid): %C = 44.40; %H = 3.32; %N = 13.61, %Cd = 21.85; %Cl = 13.80; Calc.: %C = 44.42; %H = 3.34; %N = 13.45; %Cd = 21.88; %Cl = 13.82. Yield: 83%. m.p.: >300°C. IR: $\bar{\upsilon}$ = 3250 (NH), 1641 $(C=N)_{azo}$, 802 $(C=N)_{py}$, 509 (Cd-O), 446 (Cd-N). ^{1}H NMR: d = 10.60 (s, NH), 7.24–8.45 (m, 10H/aromatic protons), 2.30 (s, 3H, –N=C–CH_3/methyl group), 3.75 (s, 3H/–OCH_3). ^{13}C NMR: d (ppm) main signals: 139 $(C=N)_{Azo}$; 150 $(C=N)_{py}$); 10 (CH_3). Molar conductivity: Λ_m = 10 ohm^{-1} cm^2 mol^{-1} (in DMSO).

$[Cu(P)(H_2O)Cl]$ (4, $CuC_{17}H_{18}N_5O_2Cl$) Found (brown solid): %C = 45.60; %H = 4.11; %N = 15.62; %Cu = 14.18; %Cl = 7.97, Calc.: %C = 45.63; %H = 4.05; %N = 15.65, %Cu = 14.20; %Cl = 7.93. Yield: 83%, m.p.: >300°C; IR: $\bar{\upsilon}$ = disappear (NH), disappear $(C=N)_{azo}$, 832 $(C=N)_{py}$, 1636 (N=N), 529 (Cu-O), 448 (Cu-N). μ_{eff} = 2.1 B.M.; band position: 14,643 cm^{-1}.

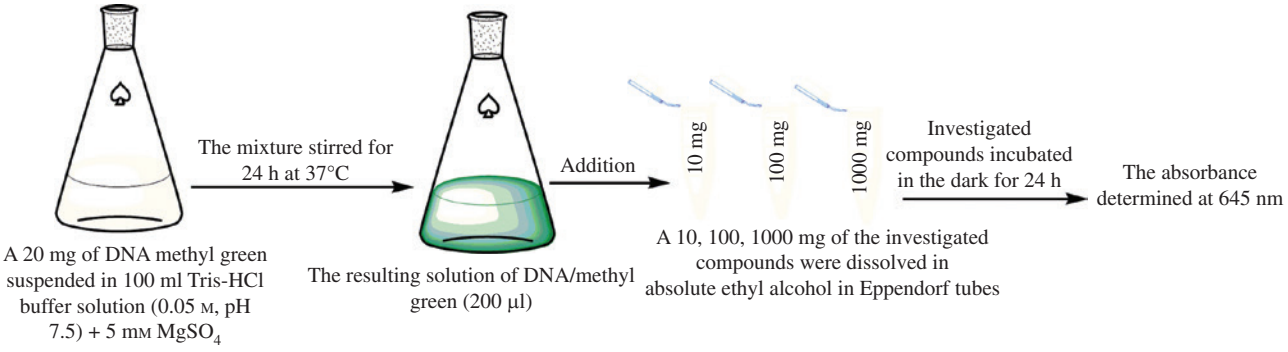

Figure 2: The steps for colorimetric assay for the investigated compounds.

ESR: $g_{//} = 2.27$, $g_{\perp} = 2.06$, $A_{//} \times 10^{-4} = 162\ cm^{-1}$, $g_{//}/A_{//} = 140$, $G = 4.2$, $\alpha^2 = 0.78$, $\beta^2 = 0.84$. Molar conductivity: $\Lambda_m = 9\ ohm^{-1}\ cm^2\ mol^{-1}$ (in DMSO).

2.5 Molecular modeling

Density function theory (DFT) was applied to predict the optimized geometry of prepared complexes by using the GAUSSIAN 09 program package [18]. The DMOL3 program in Materials Studio package [19] was used to determine the cluster calculations. PBEPBE [20] is a good exchange correlation functional that is based on generalized gradient approximation [21]. Additionally, the molecular electrostatic potential (MEP) was estimated using the B3LYP/6-31G(d) [22] level of theory.

2.6 Antibacterial activity

The disc diffusion technique [23] was used to decide the minimum inhibition concentration of examined compounds against *Pseudomonas aeuroginosa* and *Escherichia coli* as a Gram (–) bacteria and *Staphylococcus aureus* and *Bacillus subtilis* as a Gram (+) bacteria; as shown in Supplementary Figure 1S. In this method, the paper discs (Whatman filter paper, no. 42, uniform diameter 2 cm) soaked in the desired concentration of the complex solutions (2 mg/ml) were placed aseptically in petri dishes containing nutrient agar media (20 g agar + 3 g beef extract + 5 g peptone) seeded with different types of bacteria. The petri dishes were incubated at 37°C and the inhibition zones were recorded after 24 h. Each treatment was replicated six times. Note that the antibacterial activity of a common standard antibiotic Ampicillin was also recorded using the same procedure as above at the same concentrations and solvent. The % activity index for the investigated complexes was calculated by applying this equation:

$$\%\ \text{activity index} = \text{zone of inhibition by test compound (diameter)}/\text{(zone of inhibition by standard (diameter)} \times 100.$$

2.7 Colorimetric assay for compounds that bind DNA

The colorimetric assay steps [24] for the investigated compounds are shown in Figure 2. The results improved for primary absorbance and stabilized as the percentage of the untreated standard.

3 Results and discussion

3.1 Infrared, MS, ^{1}H, and ^{13}C-NMR spectra

The significant infrared (IR) bands of the HP and its Zn(II), Cd(II), and Cu(II) complexes were chosen to identify the effect of the coordination of metal to the vibration of the ligand. The infrared spectrum of the HP revealed a medium-intensity broad band due to ν(NH) at 3250 cm^{-1} [25]. Also, there are two bands related to $\nu(C{=}N)_{azo}$ [26] and $\nu(C{=}N)_{py}$ [27] at 1652 and 802, respectively.

The ^{1}H-NMR spectrum of HP in DMSO displayed peaks at 10.46, 2.32, 3.83 and 7.18–8.74 ppm movable to protons of NH, –N=C–CH_3, –OCH_3, and aromatic protons, respectively.

The MS of HP exhibited a molecular ion peak $[M]^{+\cdot}$ of HP at $m/z = 331.14$ (100.0%), that is, corresponding to its molecular weight and formula ($C_{19}H_{17}N_5O$).

The ^{13}C-NMR spectrum of HP was detected in DMSO (Supplementary Figure 2S). The signals for the $(C{=}N)_{Azo}$ and 156 $(C{=}N)_{py}$ were shown at the downfield position (147 and 156, respectively).

In the IR spectra of $[Zn(HP)(OAc)_2]$ and $[Cd(HP)Cl_2]$ complexes, the $\nu(C{=}N)_{py}$ shifted to a higher frequency but the $\nu(C{=}N)_{azo}$ shifted to a lower frequency, representing the coordination of pyridine nitrogen and azomethine nitrogen. Therefore, HP worked as a neutral bidentate ligand. Likewise, new bands were detected at 464 (446) and 511 (509) cm^{-1} movable to ν(M-N) and ν(M-O), correspondingly [28]. Moreover, the $[Zn(HP)(OAc)_2]$ complex has two bands at 1345 and 1433 cm^{-1} movable to the ν_s(O-C-O) and ν_{as}(O-C-O) of the acetate group with a difference (80 cm^{-1}) that points to bidentate bonding for the acetate group [29]. In ^{1}H-NMR spectra of $[Zn(HP)(OAc)_2]$ and $[Cd(HP)Cl_2]$ complexes in DMSO, the signal was ascribed to the NH proton, representing that these groups did not participate in coordination. Furthermore, the ^{13}C-NMR

spectra of Cd(II) and Zn(II) complexes showed signals at 140 (149) and 139 (150) ppm attributed to $(C=N)_{Azo}$ and $(C=N)_{py}$, correspondingly.

However, in the case of Cu(II), the HP worked as a mononegative bidentate ligand through $\nu(C=N)_{py}$ and $\nu(-N=N-C-)_{azo}$. This manner of coordination was proposed by (a) the shift of $\nu(C=N)_{py}$ to a higher frequency; (b) the fading of $(C=N)_{azo}$ with the immediate presence of a new band at 1636 related to (N=N); and (c) the presence of new bands at 448 and 529 cm^{-1} attributable to ν(Cu-N) and ν(Cu-O), respectively [28].

3.2 Magnetic moment and electronic spectra

The magnetic moment magnitude was 2.1 BM in [Cu(P)-(H_2O)Cl] complex, which represented the existence of Cu(II) ion. The electronic spectrum displayed a broad band with a maximum at 14,643 cm^{-1} that related to $^2B_{1g}^- \rightarrow {}^2A_{1g}^-$ transitions in a square planar structure [30].

3.3 ESR studies

The ESR spectrum of the [Cu(P)(H_2O)Cl] complex at room temperature (Supplementary Figure 3S) exhibited axially symmetric g tensor parameters ($g_{//} > g > 2.0023$) wherever the magnitude of g showed a square planar around the copper (II) center where the unpaired electron existed in the $d_{x^2-y^2}$ orbital [31]. In axial symmetry, the G magnitude (4.4), which estimates the exchange interaction between Cu(II) centers in the isolated complex, was stated by

$$G = (g_{//} - 2)/(g_{\perp} - 2) = 4.$$

Therefore, according to Hathaway and Billing [32], if $G > 4$, the exchange interaction between Cu(II) centers was excluded.

The molecular orbital coefficients (β^2 and α^2) were estimated by applying these equations [33]:

$$\beta^2 = \frac{(g_{//} - 2.0023)E}{-8\lambda\alpha^2}$$

$$\alpha^2 = \left(\frac{A_{//}}{0.036}\right) + (g_{//} - 2.0023) + \frac{3(g_{\perp} - 2.0023)}{7} + 0.04$$

where β^2 is a measure of the covalent in-plane π bonding; α^2 is a covalent in-plane σ bonding; $\lambda = -828$ cm^{-1} for the free Cu(II) ion and E is the energy of electronic transition. The outcomes data indicated that the in-plane σ bonding and in-plane π bonding are noticeably ionic. These outcomes expected because there are suitable ligand orbitals to associate with the d_{xy} orbital of the Cu(II) ion. For the square planar geometry complex, the minor magnitude of β^2 related to α^2 indicated that the in-plane π bonding is more covalent than the in-plane σ bonding. This information fit reliably with other stated magnitudes [34].

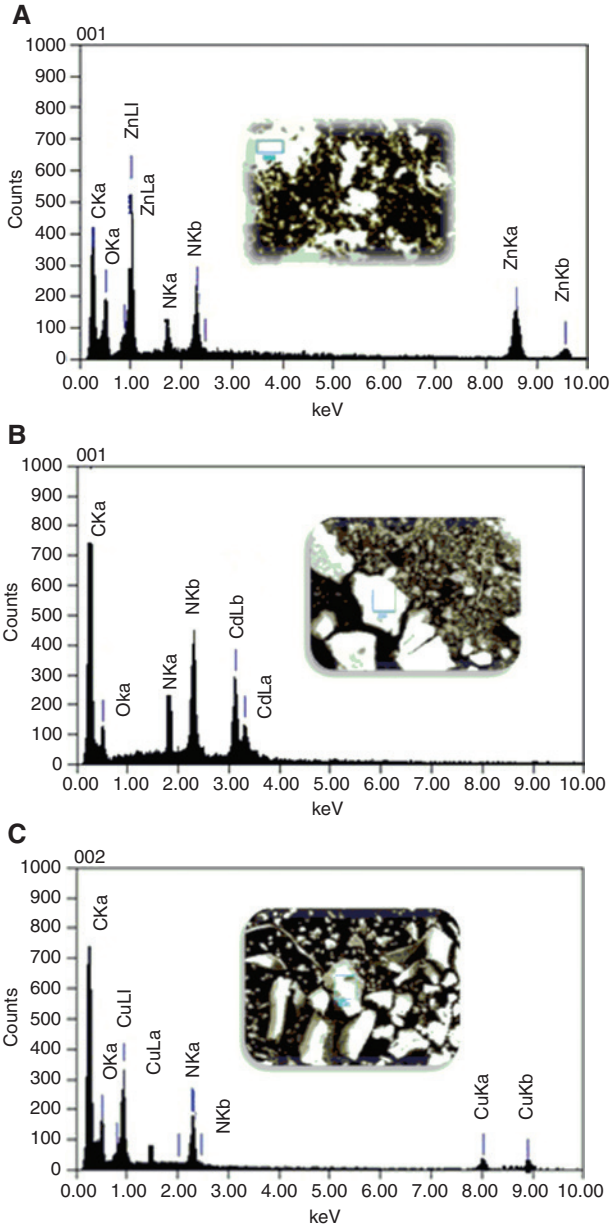

Figure 3: EDX and SEM views of (A) $[Zn(HP)(OAc)_2]$, (B) $[Cd(HP)Cl_2]$, and (C) [Cu(P)(H_2O)Cl] complexes.

Table 1: XRD data for Zn(II), Cd(II), and Cu(II) complexes.

Complex	θ°	D (Å)	FWHM (β)	S (Å)	S (nm)	I
2	21.981	2.057	0.2144	7.283	0.728	378
3	21.975	2.058	0.2033	7.682	0.768	245
4	21.965	2.059	0.2105	7.410	0.741	154

FWHM, full width at half maximum.

3.4 SEM and energy-dispersive X-rays

The surface morphologies of $[Zn(HP)(OAc)_2]$, $[Cd(HP)Cl_2]$ and $[Cu(P)(H_2O)Cl]$ complexes were estimated by using SEM, which is a potent technique for the study of surface structures. The complexes in Figure 3 show irregular broken ice rock morphologies with particle sizes of approximately a micrometer, which were randomly distributed over these ice rock–shaped structures [35].

Furthermore, the chemical compositions of Zn(II), Cd(II), and Cu(II) complexes are diverse according to energy-dispersive X-ray (EDX) spectrometer analysis, as displayed in Figure 3. The EDX figure represents the presence of carbon, nitrogen, oxygen, chloride atoms and zinc, cadmium, and copper ion in the complexes' skeletons, evidencing chelation between the ligand and the metal ion.

3.5 XRD

The Zn(II), Cd(II), and Cu(II) complexes were examined by XRD at room temperature using Cu, Kα radiation. The diffraction patterns (Supplementary Figure 4S) of the examined compounds were attained in a region of ($10° < 2\theta < 80°$) [36]. The sharp peaks displayed in the patterns indicate the formation of a well-defined distorted crystalline construction. The size of crystalline intended by using equation of Debye–Scherrer at full width at half maximum of the characteristic peaks:

$$\beta = 0.94\ \lambda/(S \cos \theta)$$

B = the line width at half maximum height

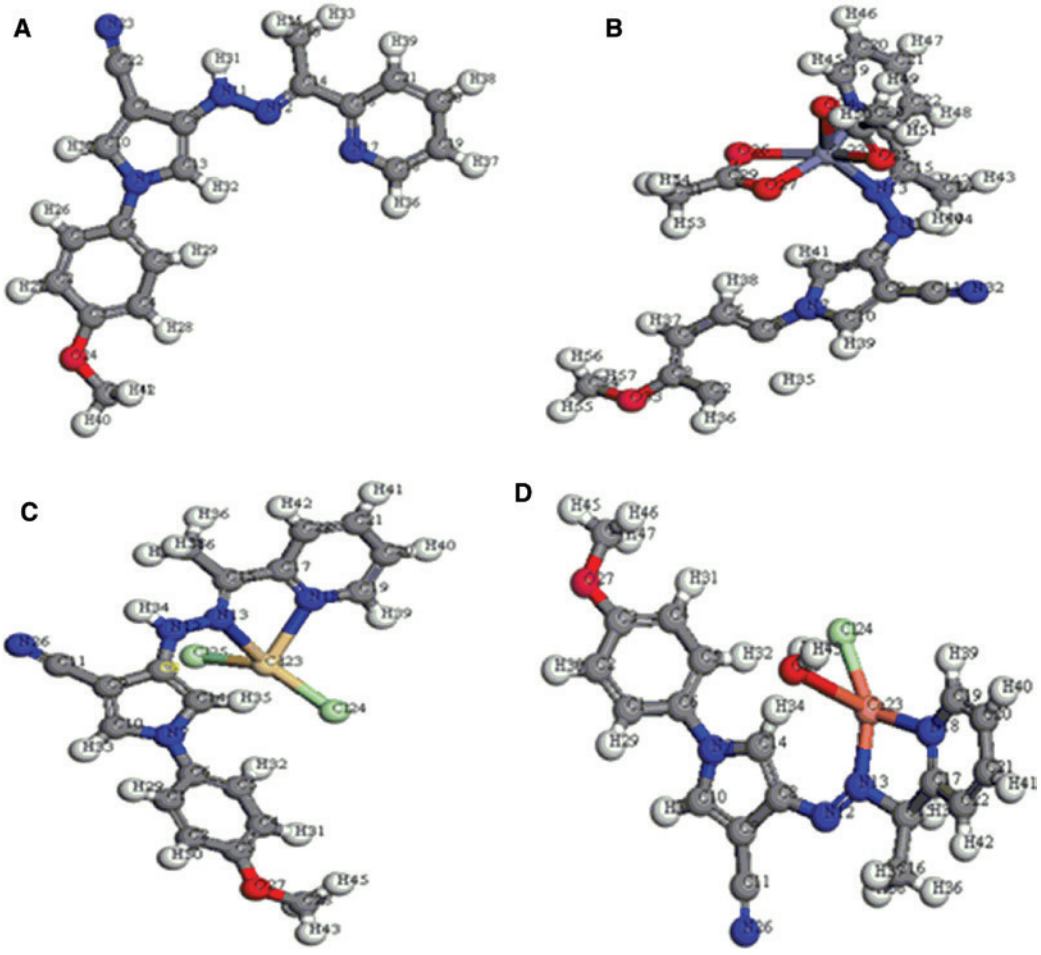

Figure 4: Molecular modeling of (A) HP, (B) $[Zn(HP)(OAc)_2]$, (C) $[Cd(HP)Cl_2]$, and (D) $[Cu(P)(H_2O)Cl]$.

$$\text{Cu/K}\alpha\ (\lambda) = 1.5406\ \text{Å}$$

S = the crystallite size

θ = the diffraction angle

Furthermore, using a Bragg equation, the magnitude of the inner crystal plane d spacing was estimated as

$$n\lambda = 2d\sin(\theta) \text{ at } n = 1$$

The magnitudes of the particle size and lattice parameters of isolated complexes are collected in Table 1. The obtained particle sizes were found in the 7.283–7.683 Å region.

3.6 DFT

The DFT was applied to optimize the geometry (Figure 4) and the quantum chemical parameters, for instance, "E_{LUMO}, E_{HOMO}, exchange-correlation, dipole moment, kinetic energy, electrostatic energy, binding energy, sum of atomic energies, spin polarization, binding energy, and total energy" (Table 2) of isolated compounds [37]. The results showed that

1. The negative magnitude of E_{LUMO} and E_{HOMO} indicated the stability of isolated complexes (Supplementary Figure 5S) [38].
2. The greater magnitude of the binding energy for isolated complexes compared with the free ligand (HP) pointed to the larger stability of the complexes compared with the ligand alone [39].
3. The higher dipole moment of complexes compared with the ligand alone indicated the potent activities of the isolated Zn(II), Cd(II), and Cu(II) complexes [39]. In addition, the electric dipole moment is an assessment of the separation of electrical charges in a molecular system.

3.7 MEP of HP

The MEP is a suitable method for the determination of good sites for nucleophilic and electrophilic attack [40]. Therefore, to obtain the MEP of isolated compounds, we should optimize the geometry of the molecular system by first applying the Becke 3LYP/6-31 G(d) level of theory. The three dimensional plots of MEP were outlined for HP and its Zn(II), Cd(II), and Cu(II) complexes as shown in Figure 5. In MEP, the green area pointed to the neutral electrostatic potential, the red area indicated the more attractive potential atoms, and the blue area indicated the more repulsive potential atoms [41].

Table 2: The molecular parameters of the of HP and its Zn(II), Cd(II), and Cu(II) complexes.

Compound	Total energy (Ha)	Sum of atomic energies (Ha)	Binding energy (Ha)	Kinetic energy (Ha)	Electrostatic energy (Ha)	Exchange correlation (Ha)	Spin polarization (Ha)	Dipole moment (Debye)	HOMO (eV)	LUMO (eV)
1	−1083.5920	−1075.9093	−7.6827	−11.7474	−1.5896	3.1348	2.51937	6.6372	−4.202	−1.650
2	−1795.8129	−1785.2378	−10.575	−15.5398	−2.1175	4.1016	2.98063	5.0795	−5.028	−3.379
3	−2093.9852	−2086.0952	−7.8900	−10.3604	−3.1937	3.3537	2.31048	4.4462	−5.156	−3.123
4	−1842.9314	−1834.7051	−8.2262	−10.8504	−3.2830	3.4631	2.44407	7.2576	−4.019	−3.158

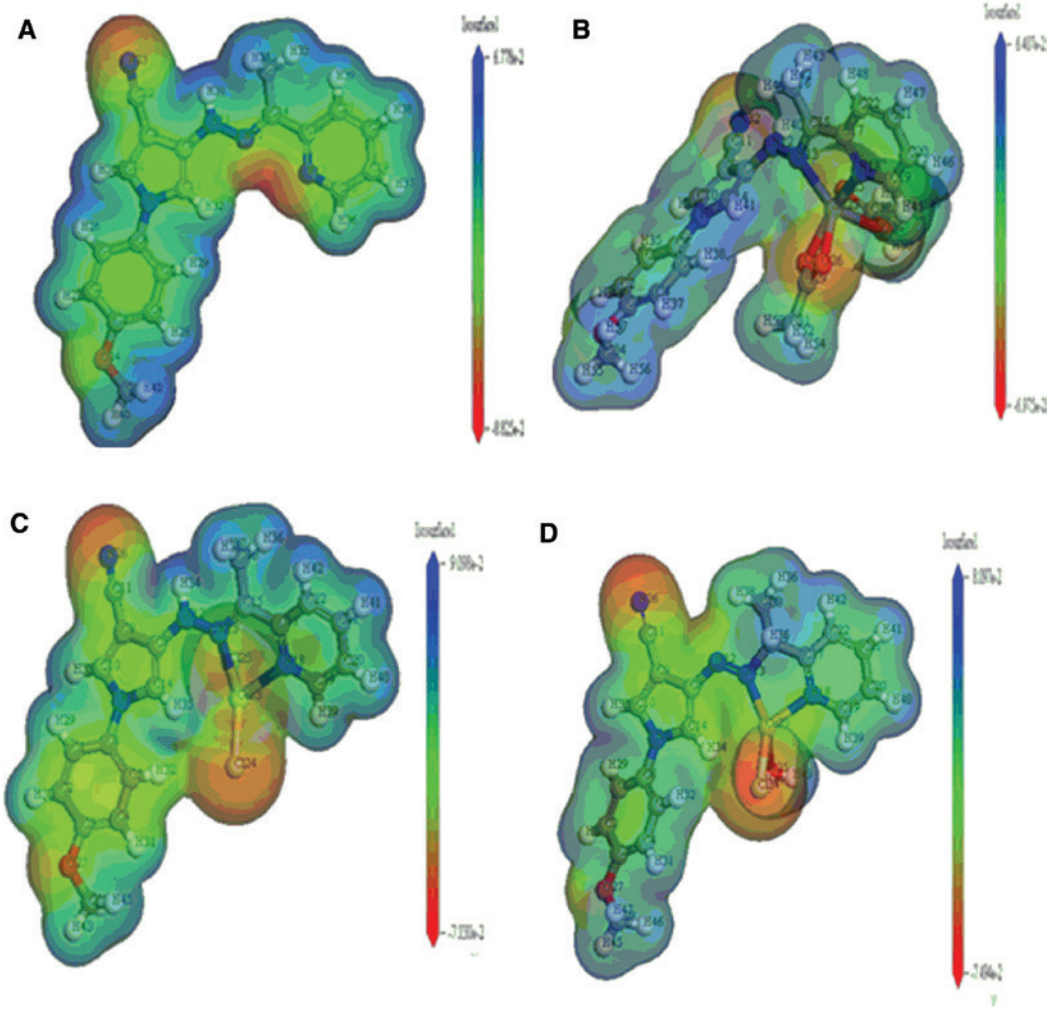

Figure 5: Molecular electrostatic potential of (A) HP, (B) $[Zn(HP)(OAc)_2]$, (C) $[Cd(HP)Cl_2]$, and (D) $[Cu(P)(H_2O)Cl]$.

3.8 Antibacterial activity

The investigated compounds, Ampicillin (standard drug) and DMSO (solvent control), were screened individually for their antibacterial activity against *P. aeuroginosa* and *E. coli* as Gram (–ve) bacteria and *B. subtilis* and *S. aureus* as Gram (+ve) bacteria [42–44]. The activity of the investigated compounds compared with the activity of Ampicillin as well as the intended percentage of activity index. The outcomes proposed that the Zn(II) and Cd(II) complexes (Table 3) had higher activity against various kinds of bacteria. We conclude that the complexes showed better antibacterial activity than the ligand (HP) alone.

Table 3: Antibacterial activity in terms of percentage of % activity index.

Compound	*E. coli*	*P. aeuroginosa*	*S. aureus*	*B. subtilis*
Ampicillin	100	100	100	100
1	66	62	57	55
2	89	93	90	89
3	87	95	93	90
4	66	67	66	63

3.9 Colorimetric assay for compounds that bind DNA

At pH 7, methyl green was reversibly binding to DNA and the colored complex was stable wherever methyl green was absent at this pH. However, the binding active compounds with DNA substituted the DNA from its methyl green complex. The movement was determined by spectrophotometric studies as a reduction in the absorbance at 630 nm. The results indicated that Zn(II) and Cd(II) complexes displayed the maximum affinity to DNA, which was recognized by absorption of the complex at the origin or by transferring for minor spaces and then evaluating the IC50 magnitude (Table 4), whereas HP and Cu(II) complex showed moderate activity.

Table 4: DNA/methyl green colorimetric assay of the DNA-binding compounds.

DNA-active compound	DNA/methyl green (IC50, µg/ml)
1	31.0 ± 2.0
2	20.3 ± 1.3
3	24.6 ± 1.9
4	34.1 ± 1.3

IC50 values represent the concentration (mean ± SD, *n* = three to five separate determinations) required for a 50% decrease in the initial absorbance of the DNA/methyl green solution.

3.10 Drug-likeness and molecular property prediction

The HP and its Zn(II), Cd(II), and Cu(II) complexes were examined for agreement with the rule of five (Table 5). The rule of Lipinski stated that "a molecule probable to develop as an orally active drug applicant presented no further than one violation of the following standards: hydrogen bond acceptors (HBA) <10, hydrogen bond donors (HBD) <5, an octanol-water partition coefficient <5, and molecular weight <500 Da" [45]. The MolSoft software was used to evaluate the drug-likeness model score and the molecular properties of the isolated compounds [46]. The calculated values of HBD and HBA for the studied compounds agreed with the Lipinski rule. Therefore, the prepared compounds had permeability properties through the living membrane. Furthermore, (log P) is a vital factor leading to inert membrane partitioning and stimulating permeability opposite its influence on solubility. Moreover, molecular weight has a great effect on drug action; however, the molecular weight increased outside a limit and the bulkiness of the compounds also increases. This will affect the drug receptor/DNA interactions. Additionally, the molecular polar surface area (PSA) is a sum of the surface polar atoms such as oxygen and nitrogen devoted hydrogen atoms in the investigated molecule.

Table 5: Calculated Lipinski parameters, PSA, and drug-likeness model score.

Compound	log P	HBA	HBD	M.W.	PSA	Drug-likeness model score
	≤5	≤10	≤5	≤500		
1	3.43	4	1	331.14	57.39	−0.55
2	2.04	6	1	514.61	61.24	−0.55
3	3.67	2	1	513.74	44.49	−0.59
4	4.41	4	2	447.42	56.85	−0.72

3.11 Structure activity relationship

The inverse relationship between the dipole moment and the activity of the investigated compounds compared with the experienced microbe was considered a good structure activity relationship study. In fact, the dipole moment is a proper parameter for detecting the excretion speed and penetration over the cell membrane. However, the lipophilic nature of the compound increases as the dipole moment decreases and thus the polarity also decreases where the permeation is stronger over the lipid film of the microbe [47], thus abolishing them further hostilely.

The outcomes presented in Tables 2, 3 and 4 show that the Zn(II) and Cd(II) complexes have a minor magnitude of dipole moment compared with the HP and Cu(II) complex, which points to their potent activities [48]. In addition, the E_{HOMO} and E_{LUMO} orbital energies correlated to the free radical scavenging activities of the antioxidant species [49]. Hypothetically, the electrophiles and nucleophiles were closely credited with radical scavenging activities recognized under the relative energy influence of the (HOMO/LUMO) orbitals. The investigated compounds that have low ionization energy gave up electrons simply and therefore probably share chemical reactions. The investigated compound had a sizable E_{HOMO} and insignificant E_{LUMO} values and, therefore, little ΔE (energy gab) ordered as good electron-releasing species. The potent antioxidants in this research for Zn(II) and Cd(II) complexes showed the lowest ΔE (E_{LUMO}–E_{HOMO}) values [50].

4 Conclusions

In the current study, Zn(II), Cd(II), and Cu(II) complexes with (HP) were synthesized and characterized. The outcomes from spectroscopic examinations showed that the HP worked as a neutral and/or mononegative bidentate ligand. The ESR as well as electronic spectra suggested a square planar geometry for the Cu(II) complex. In addition, the molecular modeling of isolated compounds was predicted by the DFT method. Furthermore, the biological activity of the examined compounds indicated that Zn(II) and Cd(II) have higher activities.

References

[1] Sun RWY, Zhang M, Li D, Li M, Wong AST. *J. Inorg. Biochem.* 2016, 163, 1–7.
[2] Ganguly R, Sreenivasulu B, Jagadese JV. *Coord. Chem. Rev.* 2008, 252, 1027–1050.

[3] Massai L, Pratesi A, Bogojeski J, Banchini M, Pillozzi S, Messori L, Bugarčić ŽD. *J. Inorg. Biochem*. 2016, 165, 1–6.
[4] Choi AW, Liu HW, Lo KK. *J. Inorg. Biochem*. 2015, 148, 2–10.
[5] Bottari B, Maccari R, Monforte F, Ottanà R, Rotondo E, Vigorita MG. *Bioorg. Med. Chem. Lett*. 2001, 11, 301–303.
[6] Cockerill FR, Uh JR, Temesgen Z, Zhang Y, Stockman L, Roberts GD, Williams DL, Kline BC. *J. Infect. Dis*. 1995, 171, 240–245.
[7] Mali RK, Somani RR, Toraskar MP, Mali KK, Naik PP, Shirodkar PY. *Int. J. Chem. Tech. Res*. 2009, 1, 168–173.
[8] Sidhaye RV, Dhanawade AE, Manasa K, Aishwarya G. *Curr. Pharm. Res*. 2011, 1, 135–139.
[9] Dabholkar VV, Gandhale SN, Shinde NB. *Der Pharma Chemica* 2012, 4, 320–328.
[10] Zhong-Yan HAO, Qi-Wan LIU, Jun XU, Lei JIA, Shao-Bai LI. *Chem. Pharm. Bull*. 2010, 58, 1306–1312.
[11] Ibrahim KM, Gabr IM, Zaky RR. *J. Coord. Chem*. 2009, 62, 1100–1116.
[12] Ranu BC, Stolle A. *Ball Milling towards Green Synthesis: Applications, Projects, Challenges*, RSC: Cambridge, England, 2014.
[13] Sim Y, Shi YX, Ganguly R, Li Y, García F. *Chem. Eur. J*. 2017, 23, 11279–11285.
[14] Rightmire NR, Bruns DL, Hanusa TP, Brennessel WW. *Organometallics* 2016, 35, 1698–1706.
[15] Fekri A, Zaky RR. *Spectrochimica. Acta Part A* 2014, 132, 846–853.
[16] Zaky RR, Fekri A. *J. Mol. Struct*. 2015, 1079, 203–213.
[17] Fekri A, Zaky RR. *J. Organomet. Chem*. 2016, 818, 15–27.
[18] Modeling and Simulation Solutions for Chemicals and Materials Research, Materials Studio (Version 5.0), Accelrys Software Inc., San Diego, USA. Available online at: www.accelrys.com, 2009.
[19] Zhao Y, Geng WT, Freeman AJ, Delley B. *Phys. Rev. B* 2002, 65, 11–15.
[20] Matveev A, Staufer M, Mayer M, Rösch N. *Int. J. Quantum Chem*. 1999, 75, 863–873.
[21] Hammer B, Hansen LB, Nørskov JK. *Phys. Rev. B* 1999, 59, 7413–7421.
[22] Silva-Júnior EF, Silva DL, Santos-Júnior PFS, Nascimento IJS, Silva SWD, Balliano TL, Aquino TM, Araújo-JúniorJX. *J. Chem. Pharm. Res*. 2016, 8, 279–286.
[23] Jayasree S, Aravindakshan KK. *Trans. Met. Chem*. 1993, 18, 85–88.
[24] Burres N, Frigo A, Rasmussen R, McAlpine J. *J. Nat. Prod*. 1992, 55, 1582–1587.
[25] Ibrahim KM, Gabr IM, Abu El-Reash GM, Zaky RR. *Monatsh. Fur. Chem*. 2009, 140, 625–632.
[26] Pretsch E, Bühlmann P, Badertscher M. *Structure Determination of Organic Compounds*, 4th ed., Springer: Berlin, Heidelberg, 2009.
[27] Ibrahim KM, Zaky RR, Gomaa EA, El-Hady MN. *Res. J. Pharm. Biol. Chem*. 2011, 2, 391–404.
[28] Zaky RR. *Phosphorus, Sulfur, Silicon Relat. Elem*. 2011, 186, 365–380.
[29] Zaky RR, Ibrahim KM, Gabr IM. *Spectrochim. Acta. A* 2011, 81, 28–34.
[30] Cotton FA, Wilkinson G, Murillo CA, Bochmann M. *Advanced Inorganic Chemistry*, 6th ed., American Chemical Society, John Wiley & Sons, Inc.: Hoboken, NJ, USA, 2003.
[31] Speier G, Csihony J, Whalen AM, Pierpont CG. *Inorg. Chem*. 1996, 35, 3519–3535.
[32] Hathaway BJ, Billing DE. *Coord. Chem. Rev*. 1970, 5, 143–207.
[33] Ray RK, Kauffman GR. *Inorg. Chem. Acta* 1990, 173, 207–214.
[34] John RP. *Spectrochim. Acta A* 2003, 13, 1349–1358.
[35] Lever ABP. *Inorganic Electronic Spectroscopy*, Elsevier: Amsterdam, 1968.
[36] Khan MI, Khan A, Hussain I, Khan MA, Gul S, Iqbal M, Rahman IU, Khuda F. *Inorg. Chem. Commun*. 2013, 35, 104–109.
[37] Geerlings P, De Proft F, Langenaeker W. *Chem. Rev*. 2003, 103, 1793–1812.
[38] Yousef TA, Abu El-Reash GM, El Morshedy RM. *Polyhedron* 2012, 45, 71–85.
[39] Aljahdali M, EL-Sherif AA. *Inorg. Chim. Acta* 2013, 407, 58–68.
[40] Zalaoglu Y, Ulgen AT, Terzioglu C, Yildirim G. SAÜ. *Fen. Bilimleri. Dergisi*. 2010, 14, 66–76.
[41] Tanak H, Köysal Y, Işık Ş, Yaman H, Ahsen V. *Bull. Korean Chem. Soc*. 2011, 32, 673–680.
[42] Johari RB, Sharma RC. *J. Indian Chem. Soc*. 1988, 65, 793–794.
[43] Abd El-Wahab ZH, El-Sarrag MR. *Spectrochim. Acta A* 2004, 60, 271–277.
[44] Panchal PK, Parekh HM, Patel MN. *Toxicol. Environ. Chem*. 2005, 87, 313–320.
[45] Lipinski CA, Lombardo L, Dominy BW, Feeney PJ. *Adv. Drug Deliv. Rev*. 2001, 46, 3–26.
[46] Drug-likeness and molecular property prediction, available from: http://www.molsoft.com/mprop/.
[47] Carcelli M, Mazza P, Pelizzi C, Pelizzi G, Zani F. *J. Inorg. Biochem*. 1995, 57, 43–62.
[48] El-Tabl AS, El-Saied FA, Al-Hakimi AN. *J. Coord. Chem*. 2008, 61, 2380–2401.
[49] Kohen R, Gati I. *Toxicology* 2000, 148, 149–157.
[50] Gacche RN, Jadhav SG. *J. Exp. Clin. Med*. 2012, 4, 165–169.

Supplementary Material: The online version of this article offers supplementary material (https://doi.org/10.1515/gps-2017-0057).